Ligand Binding and Protein Dynamics: A Fluorescence Depolarization Study of Aspartate Transcarbamylase from *Escherichia coli*†

C. A. Royer,‡ P. Tauc,‡ G. Hervé,‡ and J.-C. Brochon*,§

Laboratoire d'Enzymologie du CNRS, 91190 Gif-sur-Yvette, France, and Laboratoire pour l'Utilisation du Rayonnement Electromagnétique, CNRS-MEN-CEA, Université Paris-Sud, 91405 Orsay, France

Received December 22, 1986; Revised Manuscript Received April 24, 1987

ABSTRACT: The polarization of the fluorescence and the real-time fluorescence intensity decay of the two tryptophan residues of aspartate transcarbamylase from *Escherichia coli* were studied as a function of temperature. The protein was dissolved in an 80% glycerol/buffer mixture, and temperatures were varied between −40 and 20 °C in order to limit the depolarization to local rotations of the tryptophans. Two fluorescent species contribute to over 95% of the emission. They differ in their fluorescence lifetimes by approximately 4 ns depending upon the temperature observed and their fractional contributions to the total intensity. The *Y*-plot analysis of the polarization and lifetime data allows for the distinction of two rotational species by their critical amplitude of rotation, the first being component 1 and the second being component 2. We suggest that these two species correspond to the two tryptophan residues of the protein. The polarization and lifetime experiments were carried out for ATCase in presence of the bisubstrate analogue *N*-(phosphonoacetyl)-L-aspartate (PALA) and in presence of the nucleotide effector molecules ATP and CTP. The binding of PALA results in an increase in the thermal coefficient of frictional resistance to rotation of tryptophan 1 and a decrease in that of tryptophan 2. ATP binding does not affect the degree to which the protein hinders tryptophan rotation but does result in a change in the critical amplitude of rotation of tryptophan 2. The results obtained in the presence of CTP are similar to those obtained with PALA.

Aspartate transcarbamylase (ATCase)[1] from *Escherichia coli* is the first enzyme in the pyrimidine nucleotide biosynthetic pathway. It catalyzes the formation of carbamyl aspartate from carbamyl phosphate and aspartate. It is feedback inhibited by the end product CTP and activated by the purine nucleotide ATP. In addition, ATCase presents homotropic cooperativity with respect to the substrate aspartate. For reviews of the properties of ATCase, see Jacobson and Stark (1973a), Kantrowitz et al. (1980a,b), and Hervé (1987).

The quaternary structure of the enzyme is relatively complex. Two catalytic trimers bind three regulatory dimers to form the native species of 310 kDa. While the catalytic trimers retain their activity in absence of the regulatory subunits, the substrate-induced cooperativity requires the native structure. The allosteric effectors ATP and CTP bind the regulatory subunits and induce the activation or inhibition of enzyme activity (heterotropic effects). PALA, *N*-(phosphonoacetyl)-L-aspartate, is a bisubstrate analogue inhibitor that binds with high affinity the active sites at the interface between catalytic subunits and induces the homotropic transition (Collins & Stark, 1971; Jacobson & Stark, 1973b).

While the enzymatic properties of ATCase have been well characterized and its crystal structure in the absence and in the presence of PALA has been determined (Hontzako et al., 1982; Krause et al., 1987), the physical mechanisms of its allosteric regulation remain unclear. Both enzyme activity and enzyme regulation necessarily imply motion of the amino acid residues of the protein matrix. In fact, the dynamic character of proteins has been revealed in recent years (Lakowicz & Weber, 1973; Woodward et al., 1982; Lakowicz et al., 1982; Eftink, 1983; Ichiye & Karplus, 1983). Our primary concern in the following study of the dynamics of the intrinsic tryptophan residues in ATCase is to compare the dynamic properties observed for the native, unliganded enzyme with those obtained in the presence of PALA and the allosteric effectors ATP and CTP.

The dynamics of protein matrices can be probed on the nanosecond time scale through the study of the polarization of fluorescence of the intrinsic tryptophan residues. ATCase contains two tryptophans per catalytic subunit at positions 209 and 284 and only tyrosine residues per regulatory subunit as determined by amino acid and DNA sequences (Weber, 1968; Hoover et al., 1983; Konigsberg & Henderson, 1983; Schachman et al., 1984). Crystallographic studies have shown that while tryptophan-284 is relatively close to Cys-47 in the nearest catalytic site (22 Å), Trp-209 is found at 39 Å from the nearest active site. In addition, the nearest regulatory binding site is found at a distance of 54 Å from Trp-209 and 51 Å from Trp-284 (Hontzako et al., 1982).[2] It was previously reported that neither the average lifetime of tryptophan nor polarization was significantly altered by the binding of the ligands (Maliwal et al., 1984).

Using time-resolved fluorescence spectroscopy, we have resolved the data for the contributions of the two tryptophan residues. In order to isolate local tryptophan motions from domain fluctuations and overall protein tumbling, measure-

† This work was supported by Grant 83.C.1006 (Interface Physique-Biologie) of the Ministère de l'Industrie et de la Recherche to J.-C.B. and a temporary postdoctoral fellowship from the CNRS to C.A.R.

* Author to whom correspondence should be addressed.

‡ Laboratoire d'Enzymologie du CNRS.

§ Laboratoire pour l'Utilisation du Rayonnement Electromagnétique.

[1] Abbreviations: ATCase, aspartate transcarbamylase; ATP, adenosine 5′-triphosphate; CTP, cytidine 5′-triphosphate; PALA, *N*-(phosphonoacetyl)-L-aspartate; MOPS, 3-(*N*-morpholino)propanesulfonic acid.

[2] Distances obtained with the MANOSK molecular graphics program package on an Evans Sutherland PS300 of the Laboratoire pour l'Utilisation du Rayonnement Electromagnétique, Orsay, France, with the help of Jacqueline Cherfils and Dr. Joel Janin.

0006-2960/87/0426-6472$01.50/0

ments were carried out in 80% glycerol/buffer solutions. We have used Weber's modification (Weber et al., 1984) of the Perrin equation (Perrin, 1926), which yields the thermal coefficient of frictional resistance to rotation. In other words, this method gives an idea of the degree to which the protein matrix hinders tryptophan rotation.

These studies demonstrate that the dynamics of each tryptophan residue are affected by both PALA and nucleotide binding in spite of their distance from the binding sites. In addition, the effects of each ligand on tryptophan motions are specific in nature.

Materials and Methods

Chemicals. ATP (sodium salt) and CTP (sodium salt) were purchased from Sigma Chemical Co. (St. Louis, MO). *N*-(Phosphonoacetyl)-L-aspartate was a generous gift from Drs. V. Narayanan and L. Kedda of the Drug Synthesis and Chemistry Branch, Division of Cancer Treatment, NIH, Silver Spring, MD, and was added to the ATCase solution for a final concentration of 3.3×10^{-4} M. In order to ensure saturation of the regulatory sites, nucleotides were used at a final concentration of 5 mM (Windlund-Gray et al., 1973; Allewell et al., 1975).

Enzyme Preparations. ATCase was prepared according to Gerhart and Holoubeck (1967). Enzyme solutions were made dimer free by gel filtration on a LKB Ultragel ACA 22 column (Moody et al., 1979). The ATCase concentration was determined spectrophotometrically by assuming an extinction coefficient of 0.59 cm^2 mg^{-1} at 280 nm (Gerhart & Holoubeck, 1967). ATCase was extensively dialyzed at pH 7 against 50 mM MOPS Ultral from Calbiochem-Behring and diluted to 1×10^{-5} M with Gold Label glycerol from Aldrich for a final 80% weight by weight glycerol content.

Enzymatic Assay. ATCase activity was determined by the method of Porter et al. (1969) under the conditions previously described (Perbal & Hervé, 1972) in the presence of 5 mM carbamyl phosphate. ATP and CTP nucleotide solutions were controlled by UV absorption spectroscopy and thin-layer chromatography according to Beck and Howlett (1977).

Instrumentation. The temperature in the cuvette holder was regulated to ±0.1 °C with a F50 HC circulating temperature bath from Julabo and was measured also to ±0.1 °C with a microtemperature probe and digital thermometer from Bailey, Inc.

Total fluorescence and polarizations were measured in the L format on a steady-state SLM 8000 spectrofluorometer. The exciting wavelength was 305 ± 4 nm, and emission was monitored at 335 ± 4 nm. Background counts were less than 5% of the total intensity. Three measurements over 20 s each were taken and averaged from each data point, and the average scatter of the measurements was ±0.0013 polarization unit. Polarization data were converted to anisotropy with the relation

$$A = (2/3)(1/p - 1/3)^{-1} \quad (1)$$

Lifetimes were measured by the time-correlated single photon counting technique (Ware, 1971; Yguerabide, 1972; Wahl, 1975). The experimental setup has been previously described (Jameson & Alpert, 1979; Brochon, 1980; Merola & Brochon, 1986). The excitation light pulse source was the synchrotron radiation emitted by the electron storage ring ACO used in the single bunch mode with a repetition rate of 13.6 MHz. Excitation was at 305 ± 2 nm, and the emission monochromator was set at 330 ± 2 nm to avoid Raman scattering. Fluorescence decay curves were analyzed by a nonlinear least-squares method (Grinvald & Steinberg, 1974; McKinnon et al., 1977).

Data Analysis. Weber and co-workers (Weber et al., 1984; Scarlata et al., 1984; Rholam et al., 1984) have recently presented a novel approach to the study of fluorescent dye motions in solvents and proteins. In practice, they modified the Perrin (1926) equation by assuming that the viscosity term could be expanded with temperature around 0 °C:

$$\eta = \eta_0 \exp[b(T_0 - T)] \quad (2)$$

where η_0 is the viscosity at T_0 (0 °C) and b is the thermal coefficient of the viscosity.

Replacing this expression for η in the Perrin equation and taking natural logs yield

$$Y = \ln [(A_0/A) - 1] - \ln (RT\tau/V) = -\ln \eta_0 + b(T - T_0) \quad (3)$$

where A_0 is the limiting anisotropy, A is the value of the anisotropy at each Kelvin temperature T, R is the gas constant, τ is the fluorescence lifetime at each temperature, and V is the rotational volume. A plot of Y vs. T thus has a slope of b, the thermal coefficient of resistance to a rotation, and an intercept of $-\ln \eta_0$. (The limiting anisotropy and rotatinal volume were calculated by linear least-squares analyses of the low-temperature conventional Perrin plots.)

For fluorophores in pure solvents, Y vs. T is thus a straight line, the slope of which is dependent upon the viscosity of the solvant (Weber et al., 1984). For 80% glycerol the slope is approximately 7–8% and agrees well with the flow results of Miner and Dalton (1953). For tryptophan and tyrosine motions in peptides and proteins, in 80% glycerol (Scarlata et al., 1984; Rholam et al., 1984), these authors found that at low temperatures Y vs. T had the slope b_s, or solvent slope (7–8%), but that at a given temperature, T_c or critical temperature, specific to each protein, there occurred a break in the Y plot at which protein–solvent interactions ceased to be important and intraprotein interactions dominate. The second or protein slope, b_u, depends upon of the viscosity of the protein medium surrounding the tryptophan and upon the specific interactions of the tryptophan with its neighboring amino acid residues. The average angle of rotation at the critical temperatures calculated with (Perrin, 1936)

$$\cos^2 \theta = (1/3)[1 + (2A/A_0)] \quad (4)$$

is indicative of the free space surrounding the fluorophore (Scarlata et al., 1984). For proteins with two intrinsic fluorophores, three slopes, one solvant slope b_s, and two protein slopes b_1 and b_2 are observed if the critical temperatures T_{c1} and T_{c2} are sufficiently separated and if the values of b_1 and b_2 are sufficiently different. The value of b_1 is a linear-weighted combination at each temperature of the protein slope of the first tryptophan b_{u1} and the solvent slope of the second:

$$b_1 = f_1 b_{u1} + f_2 b_s \quad (5)$$

Similarly, the second slope b_2 is a linear-weighted combination of the two protein slopes, b_{u1} and b_{u2}:

$$b_2 = f_1 b_{u1} + f_2 b_{u2} \quad (6)$$

f_1 and f_2 are the fractional contributions (see below) of each tryptophan to the total fluorescence intensity at each temperature. Fluorescence intensities of components 1 and 2 were obtained by multiplying the total steady-state intensity at a given temperature by the corresponding fractional contribution. Polarization was measured every 2 deg and lifetime (and fractional contribution values) at intervals of 5 deg. The variation of anisotropy, A, lifetime, τ and the fractional contribution, f_1, were fitted and interpolated every 1 deg with a polynomial approximation. Fluorescence decay curves were

Table I: Analysis of Fluorescence Decays of ATCase–ATP as a Biexponential or a Sum of Three Exponential Components[a]

T (°C)	τ_1 (ns)	c_1, f_1 (%)	τ_2 (ns)	c_2, f_2 (%)	τ_s (ns)	c_s, f_s (%)	χ^2
−36.5	6.41	0.677, 81.7	3.01	0.323, 18.3			3.44
	6.68	0.036, 70.7	3.75	0.026, 28.7	<0.01	0.938, 0.6	2.22
−17.6	6.00	0.611, 77.5	2.74	0.389, 22.5			2.40
	6.08	0.007, 73.5	3.01	0.005, 26.2	<0.01	0.988, 0.3	2.00
−10.1	5.76	0.452, 70.0	3.00	0.548, 30.0			2.25
	5.81	0.007, 68.0	3.09	0.006, 32.0	<0.01	0.987, <0.1	2.17
10.1	5.09	0.303, 45.6	2.64	0.697, 54.4			2.45
	5.21	0.022, 41.5	2.73	0.058, 58.1	<0.01	0.920, 0.4	2.21

[a] c_i are the relative coefficients of the exponential terms, and f_i are the fractional contributions to the total fluorescence emission as respectively defined in eq 8 and 9. The subscript s is devoted to the short-lifetime component. Associated errors are typically 0.01 ns for τ_1 and τ_2 and 0.001 for the coefficients c_i.

correctly fitted with a correlation of a sum of three exponentials with the exciting pulse profile as follows:

$$I(t) = \int_0^t g(u)f(t-u)\,du \tag{7}$$

with

$$f(t) = \sum_i^n c_i \exp(-t/\tau_i) \tag{8}$$

and

$$\sum c_i = 1$$

The fractional contribution of each exponential component i to the total fluorescence intensity is given by

$$f_i = \frac{\int_0^\infty c_i \exp(-t/\tau_i)\,dt}{\sum_{i=1}^n \int_0^\infty c_i \exp(-t/\tau_i)\,dt} \tag{9}$$

The best fit was achieved with three components, the first two of which represented over 95% of the emission (see Table I for an example). These two components had lifetimes between 2 and 7 ns, depending upon the temperature, while the third component was very short. The long-lifetime fractional components, c_1 and c_2, were normalized, and the third short-lifetime component, τ_s, was neglected in the following analysis. In Y-plot calculations τ_m, the average fluorescence lifetime (calculated from $f_1\tau_1 + f_2\tau_2$), was used. This approximation is justified by the very low contribution to the total depolarization of a fluorescent species with such a short decay time. In addition, the real-time fluoresence anisotropy decay showed no evidence for a very fast rotation.

Experimental values of b_s, b_1, and b_2 were determined from a least-squares linear regression of the data points. The experimental values of b_s were used in eq 5 along with the values of f_1 and f_2 at each temperature for the determination of b_{u1}. This value was in turn used in eq 6 for the determination of b_{u2}. Because the values of f_1 and f_2 change with temperature above 0 °C, the value of b_2 used in eq 6 was the result of a sliding nearest-neighbor linear regression every 3 deg.

Results

Analysis of Fluorescence Emission Heterogeneity of ATCase as a Function of Temperature. The analysis of the fluorescence decay curves for ATCase in 80% glycerol at all temperatures yields three fluorescent species. Curves at four different temperatures are shown in Figure 1. The first component has a lifetime between 10 and 300 ps depending upon the temperature, and its fractional contribution never exceeded 4.5%. Background measurements have shown that this component is not due to Raman scattering, and its very short lifetime makes its contribution to the depolarization

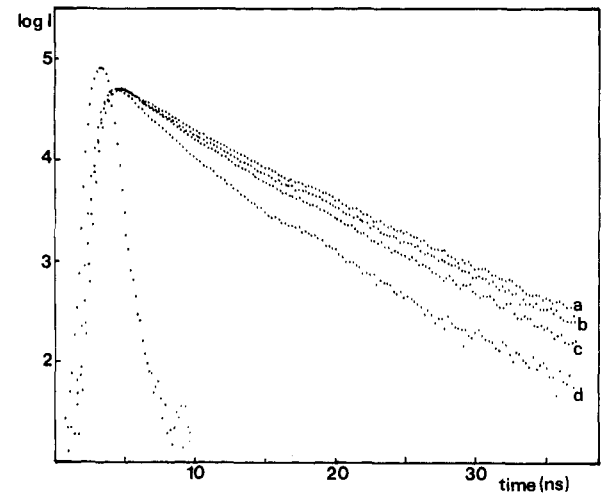

FIGURE 1: Fluorescence intensity decay curves for ATCase in presence of ATP; log intensity vs. time (ns). (a) −36.4 °C; (b) −17.6 °C; (c) −10.1 °C; (d) 10.0 °C.

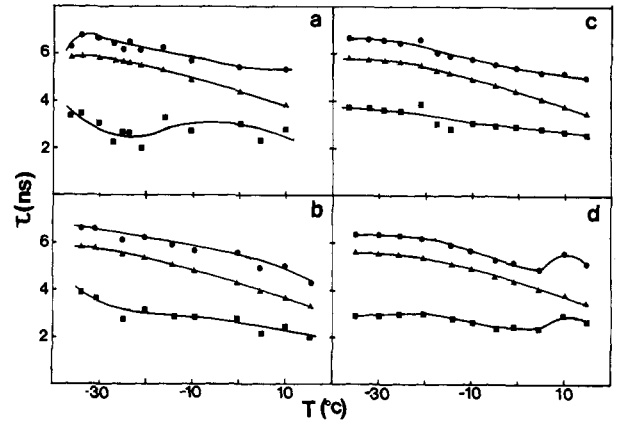

FIGURE 2: Fluorescence lifetime, τ (ns), vs. temperature (°C). (●) Component 1, (■) component 2, and (▲) mean lifetime τ_m for (a) ATCase, (b) ATCase in presence of PALA, (c) ATCase in presence of ATP, and (d) ATCase in presence of CTP.

negligible. The two other components are thus responsible for more than 95% of the emission. The sum of the fractional contributions of these components were normalized. Their lifetime temperature profiles as well as those of the mean lifetime, τ_m, for ATCase alone and in presence of each of its three ligands are shown in Figure 2. The lifetime vs. temperature profiles of each component are not in all cases a monotonous function of temperature (i.e., the case of ATCase and ATCase in presence of CTP). However, the mean lifetime profiles, τ_m, were easily fit with a polynomial of second degree.

The fractional contributions of the two major components (1, long lifetime; 2, short lifetime) are plotted in Figure 3 as a function of temperature for all four solutions studied. The profiles for ATCase and ATCase + PALA are similar, with

Table II: *Y*-Plot Parameters for ATCase

	A_0	V (mL/mol)	T_{c1} (°C)	T_{c2} (°C)	θT_{c1} (deg of arc)	θT_{c2} (deg of arc)	b_s (%)	b_1 (%)	b_2 (%)	b_{u1} (%)	b_{u2} (%)
ATCase	0.3209	119	−32	−24	6.5	7.9	8.5	4.9	3.8	3.8	3.9
ATCase + PALA	0.3202	174	−32	−20	5.4	7.6	8.8	6.2	4.5	5.5	2.9
ATCase + ATP	0.3243	143	−33	−17	5.8	8.9	9.2	5.4	4.1	4.1	4.0
ATCase + CTP	0.3283	120	−32	−24	6.4	7.8	8.9	5.7	3.9	5.1	1.7

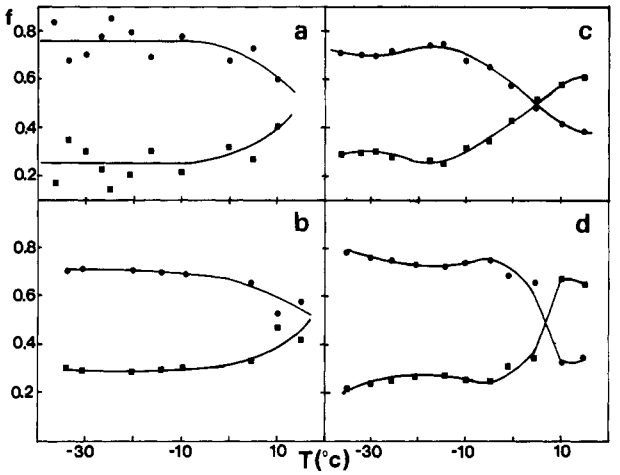

FIGURE 3: Fractional contributions to the total fluorescence emission (f) vs. temperature (°C). (●) Component 1 and (■) component 2 for (a) ATCase, (b) ATCase in presence of PALA, (c) ATCase in presence of ATP, and (d) ATCase in presence of CTP.

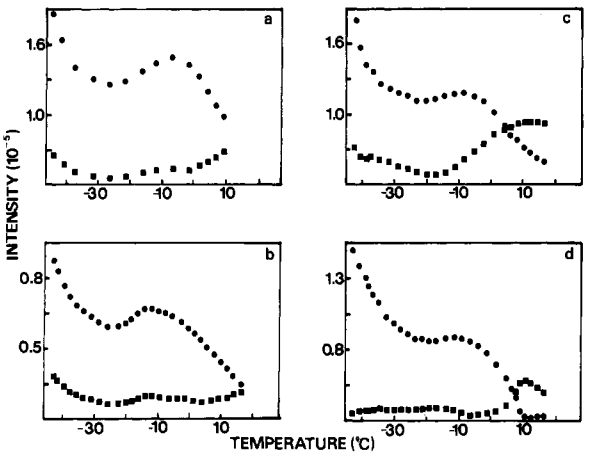

FIGURE 4: Fluorescence intensities vs. temperature (°C). (●) Component 1 and (■) component 2 for (a) ATCase, (b) ATCase in presence of PALA, (c) ATCase in presence of ATP, and (d) ATCase in presence of CTP.

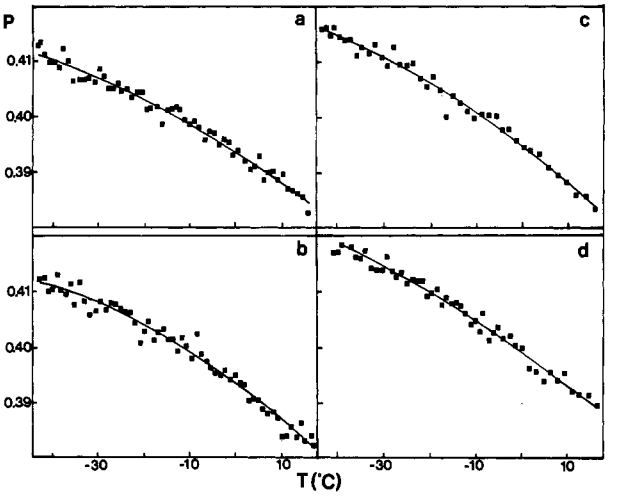

FIGURE 5: Fluorescence polarization (P) vs. temperature (°C) for (a) ATCase, (b) ATCase in presence of PALA, (c) ATCase in presence of ATP, and (d) ATCase in presence of CTP.

the two fractions practically equal at approximately 15 °C. In presence of nucleotides, f_1 and f_2 are inversed at approximately 0 °C for ATCase in presence of ATP and 5 °C in presence of CTP.

In Figure 4 are plotted the fluorescence intensities of each component as a function of temperature. The profile of component 1 (the long-lifetime component) is not at all a monotonous function of temperature. From −40 to approximately −20 °C, depending upon the state of ligation, the fluorescence is quenched by increasing temperature. Between −20 and 0 °C, the intensity of component 1 increases with temperature. Above 0 °C increasing temperature once again results in quenching of component 1. One can interpret this anomalous temperature behavior as follows. Between −40 and −20 °C, increasing temperature causes an increase in motion that brings the tryptophan residue in contact with a nearby quencher. Because lifetime profiles (Figure 2) do not follow intensity profiles, we must assume ground-state complex formation. As temperature continues to increase, tryptophan motions become larger, and the probability of ground-state complex formation decreases. Finally, motions continue to increase, collisional quenching becomes more important, and just as lifetime decreases so does intensity. Another possible explanation could involve temperature-induced shifts in the spectral energy such as those observed for fluorophores in polar solvents (Macgregor & Weber, 1981). However, the normalized emission spectra recorded as a function of temperature (not shown) demonstrate that by monitoring at the emission maximum (335 nm) there is virtually no decrease in intensity at this wavelength in spite of the red shift upon increasing temperature from −36.5 to 10 °C. Component 2 also has an interesting intensity vs. temperature profile with a decrease in intensity between −40 and −20 °C and a slight increase at higher temperatures.

The fluorescence intensity profiles for both components reflect the fractional contribution data for the four solutions studied. The intensity values become equal for ATCase and ATCase + PALA around 15 °C but cross at lower temperatures in presence of nucleotides (between 0 and 5 °C). Component 2 shows a large increase in intensity when ATP is present, and the low-temperature decrease in intensity of component 2 is not observed in presence of CTP.

Y vs. Temperature Plots of ATCase. In Figure 5 are presented the temperature profiles of the polarization for the four ATCase solutions. Although these profiles are not identical, this direct representation does not permit a detailed interpretation of the rotations of the tryptophan residues of this protein or of any changes that may be caused by the binding of the ligands. Likewise, the real-time anisotropy decay curves at any given temperature do not allow for resolution of the rotations of the two fluorescent species.

In contrast, Weber's representation (Weber et al., 1984) of the temperature dependence of the anisotropy data permits a much more in-depth analysis of the rotational behavior of the system. From the fitted values of A and τ_m as a function of temperature, Y vs. T was calculated from eq 3 for all four

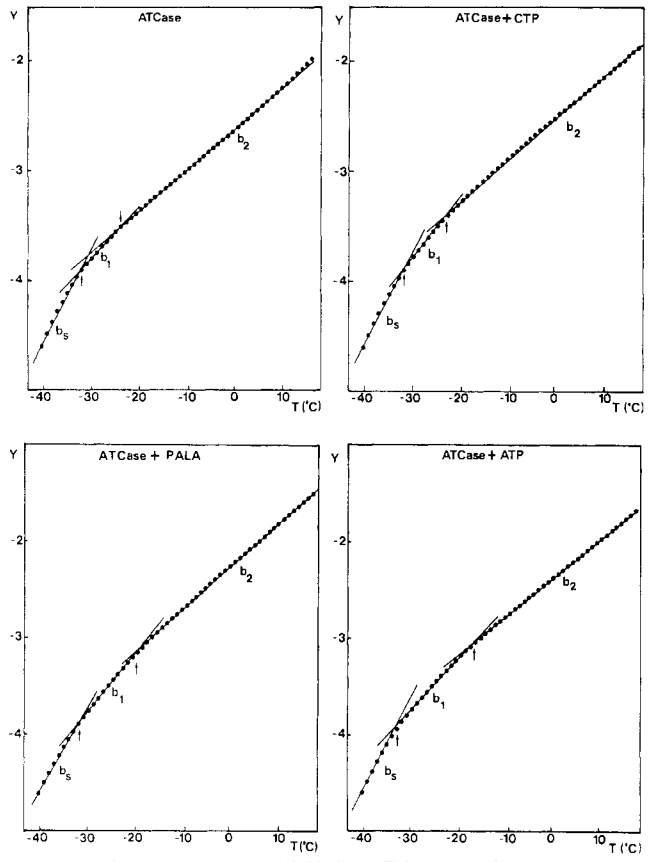

FIGURE 6: Y vs. temperature (°C) for ATCase, ATCase in presence of PALA, ATCase in presence of ATP, and ATCase in presence of CTP as labeled.

solutions studied (Figure 6). The results of the Y-plot analysis are summarized in Table II.

The first slope observed, the solvent slope b_s, is between 8.5 and 9.2% for all four plots. These values are in agreement with the results of Miner and Dalton (1953), Scarlata et al. (1984), and Rholam et al. (1984).

Another feature is common to all four plots. The first critical temperature observed, T_{c1}, is found at -32 ± 1 °C. The amplitude of rotation calculated from the values of the anisotropy at that temperature and with eq 4 yields values between 5.4° and 6.5° of arc.

A second break in the Y plot occurs for all four ATCase solutions studied. The second critical temperature for ATCase alone and ATCase bound by CTP is the same, −24 °C. When PALA is bound, T_{c2} increased to −20 °C and in presence of ATP to −17 °C. The amplitude of rotation of the second component calculated from eq 4 is altered by the binding of ATP as it increases from 7.9° to 8.9° of arc.

From the values of the fractional contribution, f_i, of each component and the values of Y as a function of temperature, b_{u1} and b_{u2} were calculated for each solution from eq 5 and 6. It was assumed that the two emitting components were independent. This assumption is supported by the high values of A_0 in all four cases, indicating that no energy transfer occurs between tryptophans as should be expected for red-edge excitation (Weber, 1960). In addition, in solving for b_{u1}, the short-lifetime component must be assumed to be component 2 (the tryptophan which below T_{c2} is still in the solvent regime). This is true because the inverse assumption yields negative values for b_{u1}.

Comparing the results in Table II for b_{u1} and b_{u2}, one can see that for unliganded ATCase these two values are roughly equivalent. This is also the case for ATCase bound by ATP. In contrast, the binding of PALA or CTP results in an increase in b_{u1} and a decrease in b_{u2}.

Discussion

ATCase contains only two tryptophan residues per catalytic chain, all six of which have been shown to be equivalent (Gibbons et al., 1976). Fluorescence intensity decay studies have shown that over 95% of emission results from two components, of long and short fluorescence lifetime respectively for component 1 and 2. The Y-plot analysis of the temperature dependence of the anisotropy yields two breaks in the Y plot and two protein regime slopes. For the purpose of our present analysis, we make the simplifying assumption that the two protein regime slopes, b_{u1} and b_{u2}, can be assigned to component 1 and component 2, respectively. This leads to the assumption that component 1 corresponds to one tryptophan in the ATCase primary structure and component 2 to the other. While it has clearly been shown that single tryptophan proteins can have several emitting components (Grinwald & Steinberg, 1976), we opt at this point for the simplest explanation. However, it should be pointed out that most of the following discussion is equally valid if one assumes that one tryptophan in two conformational states corresponds to the two major components.

In examining the values of the Y-plot parameters reported in Table II, it is important to bear in mind the large number of data points taken for each Y plot. In effect, although the average deviation for each polarization data point taken was ±0.0013 polarization unit, the large number of temperatures studied permits a much greater certainty of the values of the polarization at each temperature (approximately ±0.0005 polarization unit). Likewise, since the temperature is known to ±0.1 °C, T_c can be determined to at least ±1 °C. We assume that the values of T_c given carry an error of approximately ±0.5° of arc. Likewise, the values of b_u are assumed to carry an error of approximately ±0.5%, the variation in the experimental values of b_s. Thus, while one direct measurement of the anisotropy at any given temperature, even time resolved, will not yield detailed information about the rotations of the two tryptophan residues in ATCase, the accumulation of many points at many temperatures and the logarithmic representation allow for the differentiation of their two rotational components. The two tryptophan residues differ first of all by the average angle of free rotation. For all solutions except ATCase in presence of ATP, this difference is approximately 1.5° of arc. In presence of ATP this difference increases to 3.1° of arc.

While Trp-284 is found relatively close to the carbamyl phosphate binding site, Trp-209 is situated at a large distance. In addition, both residues are found at a large distance from the nucleotide binding site. To a certain degree then, they constitute a limited probe of the effect of ligands on protein dynamics. Since they do not interact directly with any ligand binding site, changes in their dynamics are more indicative of long-distance effects on the protein matrix.

Given the above assignments of component 1 to T_{c1} and b_{u1} and component 2 to T_{c2} and b_{u2}, and if one assumes that each component corresponds to one tryptophan residue in ATCase, then the conclusion is that they are roughly equivalent. That is, they undergo the same resistance to their rotation, caused by their surrounding protein matrix, although component 2 has slightly more free space to rotate. The binding of PALA to the active site results in the differentiation of the resistance to rotation of the two fluorophores. That of tryptophan 1 is greatly diminished whereas tryptophan 2 appears much more constrained by the protein. UV difference spectra have re-

vealed PALA-induced perturbations in tryptophan absorption, and this technique has been used to titrate the active site (Collins & Stark, 1971; Jacobson & Stark, 1973b). Replacement of the tryptophan residues in ATCase by 7-azatryptophan results in more pronounced heterotropic effects and in an increase in the efficiency of succinate activation (Gueguen et al., 1980; Foote et al., 1980). The study of mutant ATCases in which Trp-209 was replaced by various amino acids indicated that this residue plays a role in substrate binding (Smith et al., 1986). It has been postulated (Krause et al., 1987) that during the allosteric transition a hydrogen bond between Trp-209 and Asp-203 is broken. This could result in a greater freedom of motion for the tryptophan. Our component 1 may in fact be tryptophan-209 in the ATCase structure, although the similarity between the effects of CTP and PALA could be considered somewhat contradictory. One remarks a great similarity in the intensity profiles (which we assume to be dynamic in origin) for ATCase in presence of the two nucleotides. However, in contrast to CTP, ATP binding does not lead to the differentiation of the two tryptophan residues by changing their degree of coupling to the protein. Decoupling of the mechanisms of action of ATP and CTP on ATCase activity had already been observed by several investigators (Wong, 1971; Winlund-Gray et al., 1973; Heyde et al., 1973a,b; Wedler & Gasser, 1974; Chan & Enns, 1981; Kantrowicz et al., 1981; Buiz & Allewell, 1982; Silver et al., 1983; Shanley et al., 1984; Ladjimi et al., 1986). Ligand specificity, the presence or absence of the imidazole ring in this case, results in the differentiation of certain dynamic parameters (θ_{τ_c}, b_{u1}, and b_{u2}) but not others (fractional contributions).

Although the question of the nature of the relations between structure, dynamics, and biological activity in ATCase remains, these dynamic studies demonstrate that the binding of a small molecule by a large protein can have consequences on the dynamics of amino acid residues situated at a relatively large distance from the binding site. The changes observed in the dynamic parameters are both specific and very subtle in nature and may be indicative of the complexity of the mechanism by which binding information is transferred through the protein matrix.

ACKNOWLEDGMENTS

We are indebted to Drs. V. Narayanan and L. Kedda for the gift of PALA, to Dr. Joel Janin and Jacqueline Cherfils for their assistance in the calculation of the relative tryptophan positions, to the technical staff at LURE for running the Synchrotron Radiation machines during beam-time sessions, and to Dr. Bernard Alpert for the use of his SLM 8000 for steady-state polarization measurements.

Registry No. PALA, 51321-79-0; ATP, 56-65-5; CTP, 65-47-4; ATCase, 9012-49-1; L-tryptophan, 73-22-3.

REFERENCES

Allewell, N. M., Friedland, J., & Niekamp, K. (1975) *Biochemistry 14*, 224–230.

Beck, C. F., & Howlett, G. J. (1977) *J. Mol. Biol. 111*, 1–17.

Brochon, J. C. (1980) in *Protein Dynamics and Energy Transduction* (Shin'lchi, I., Ed.) pp 163–189, Taniguchi Foundation, Tokyo, Japan.

Burz, D. S., & Allewell, N. M. (1982) *Biochemistry, 21*, 6647–6655.

Chan, W. W. C., & Enns, C. A. (1981) *Can. J. Biochem. 59*, 461–468.

Collins, K. D., & Stark, G. R. (1971) *J. Biol. Chem. 246*, 6599–6605.

Eftink, M. (1983) *Biophys. J. 43*, 323–334.

Foote, J., Ikeda, D. M., & Kantrowitz, E. R. (1980) *J. Biol. Chem. 255*, 5154–5158.

Gerhart, J. C., & Holoubek, H. (1967) *J. Biol. Chem. 242*, 2886–2892.

Gibbons, I., Ritchey, J. M., & Schachman, M. K. (1976) *Biochemistry 15*, 1324–1330.

Grinvald, A., & Steinberg, I. Z. (1974) *Anal. Biochem. 59*, 583–598.

Grinvald, A., & Steinberg, I. Z. (1976) *Biochim. Biophys. Acta 427*, 663–678.

Gueguen, P., Padron, M., Perbal, B., & Hervé, G. (1980) *Biochim. Biophys. Acta 615*, 59–69.

Hervé, G. (1987) *Allosteric Enzymes* (Hervé, G., Ed.) CRC Publishing, Boca Raton, FL (in press).

Heyde, E., Nagabhushanam, A., & Venkataraman, S. (1973a) *Biochemistry 12*, 4718–4726.

Heyde, E., Nagabhushanam, A., & Venkataraman, S. (1973b) *Biochem. J. 135*, 125–132.

Hontzako, R. B., Crawford, J. L., Monaco, H. L., Ladner, J. E., Edwards, B. F. P., Evans, D. R., Warren, S. G., Wiley, D. C., Ladner, R. C., & Lipscomb, W. N. (1982) *J. Mol. Biol. 160*, 219–263.

Hoover, T. A., Roof, W. D., Foltermann, K. F., O'Donovan, G. A., Bencini, D. A., & Wild, J. R. (1983) *Proc. Natl. Acad. Sci. U.S.A. 80*, 2462–2466.

Ichiye, F., & Karplus, M. (1983) *Biochemistry 22*, 2884–2893.

Jacobson, G. R., & Stark, G. R. (1973a) *Enzymes (3rd Ed.) 9B*, 225–308.

Jacobson, G. R., & Stark, G. R. (1973b) *J. Biol. Chem. 248*, 8003–8014.

Jameson, D. M., & Alpert, B. (1979) in *Synchrotron Radiation Applied to Biophysical and Biochemical Research* (Castellani, A., & Garcia, J. F., Eds.) pp 183–201, Plenum, New York.

Kantrowitz, E. R., Pastra-Landis, S. C., & Lipscomb, W. N. (1980a) *Trends Biochem. Sci. (Pers. Ed.) 5*, 124–128.

Kantrowitz, E. R., Pastra-Landis, S. C., & Lipscomb, W. N. (1980b) *Trends Biochem. Sci. (Pers. Ed.) 6*, 150–153.

Kantrowitz, E. R., Reed, H. W., Ferraro, R. A., & Daigneault, J. P. (1981) *J. Mol. Biol. 153*, 569–587.

Konigsberg, W. H., & Henderson, L. (1983) *Proc. Natl. Acad. Sci. U.S.A. 80*, 2467–2471.

Krause, K. L., Volz, K. W., & Lipscomb, W. N. (1987) *J. Mol. Biol. 193*, 527–553.

Ladjimi, M., Ghelis, C., Feller, A., Cunin, R., Glandsdorff, N., Piérard, A., & Hervé, G. (1985) *J. Mol. Biol. 186*, 715–724.

Lakowicz, J. R., & Weber, G. (1973) *Biochemistry 12*, 4171–4179.

Lakowicz, J. R., Maliwal, B., Cherek, H., & Balter, A. (1983) *Biochemistry 22*, 1741–1752.

Macgregor, R. B. & Weber, G. (1981) *Ann. N.Y. Acad. Sci. 366*, 140–154.

Maliwal, B. P., Allewell, N. M., & Lakowicz, J. R. (1984) *Biophys. Chem. 19*, 209–216.

McKinnon, A. E., Szabo, A. G., & Miller, D. R. (1977) *J. Phys. Chem. 81*, 1564–1570.

Merola, F., & Brochon, J. C. (1986) *Eur. Biophys. J. 13*, 291–299.

Miner, M., & Dalton, N. (1953) in *Glycerol*, pp 246–286, Reinhold, New York.

Moody, M. F., Vachette, P., & Foote, A. M. (1979) *J. Mol. Biol. 133*, 517–532.

Perbal, B., & Hervé, G. (1972) *J. Mol. Biol. 70*, 511–529.

Perrin, F. (1926) *Ann. Phys. Rad. 7*, 390–401.
Perrin, F. (1936) *Acta Phys. Pol. 5*, 335–342.
Porter, R. W., Modebe, M. O., & Stark, G. R. (1969) *J. Biol. Chem. 244*, 1846–1859.
Rholam, M., Scarlata, S. F., & Weber, G. (1984) *Biochemistry 23*, 6793–6796.
Scarlata, S. F., Rholam, M., & Weber, G. (1984) *Biochemistry 23*, 6789–6792.
Schachman, H. K., Pauza, C. D., Navre, M., Karels, M. J., Wu, L., & Yang, Y. R. (1984) *Proc. Natl. Acad. Sci. U.S.A. 81*, 115–119.
Shanley, M. S., Folterman, K. F., O'Donovan, G. A., & Wild, J. R. (1984) *J. Biol. Chem. 259*, 12672–12677.
Silver, R. S., Daigneault, J. P., Teague, P. D., & Kantrowitz, E. R. (1983) *J. Mol. Biol. 168*, 729–745.
Smith, K. A., Nowlan, S. F., Middleton, S. A., O'Donovan, C., & Kantrowitz, E. R. (1986) *J. Mol. Biol. 189*, 227–238.
Wahl, P. (1975) in *New Techniques in Biophysics and Cell Biology* (Pain, M., & Smith, J., Eds.) Vol. 2, pp 233–285, Wiley, London.
Ware, W. R. (1971) in *Creation and Detection of the Excited State* (Lamola, A. A., Ed.) Vol. 1, pp 213–302, Dekker, New York.
Weber, G. (1960) *Biochem. J. 75*, 345–352.
Weber, G., Scarlata, S. F., & Rholam, M. (1984) *Biochemistry 23*, 6785–6788.
Weber, K. (1968) *Nature (London) 218*, 1116–1119.
Wedler, F. C., & Gasser, F. J. (1974) *Arch. Biochem. Biophys. 163*, 69–78.
Winlund-Gray, C., Chamberlin, M. J., & Gray, D. M. (1973) *J. Biol. Chem. 248*, 6071–6079.
Wong, G. C. (1971) Ph.D. Thesis, University of California, Davis.
Woodward, C., Simon, I., & Tuchsen, E. (1982) *Mol. Cell. Biochem. 48*, 135–139.
Yguerabide, J. (1972) *Methods Enzymol. 29*, 498–578.

Proton and Iodine-127 Nuclear Magnetic Resonance Studies on the Binding of Iodide by Lactoperoxidase†

Junji Sakurada,‡ Seizo Takahashi,§ Toru Shimizu,∥ Masahiro Hatano,∥ Shingo Nakamura,⊥ and Toichiro Hosoya*,‡

Faculty of Pharmaceutical Sciences, Chiba University, Chiba, Chiba 260, Japan, Department of Chemistry, Japan Women's University, Bunkyo-ku, Tokyo 112, Japan, Chemical Research Institute of Non-Aqueous Solutions, Tohoku University, Sendai, Miyagi 980, Japan, and Department of Agriculture, Hirosaki University, Hirosaki, Aomori 036, Japan

Received March 18, 1987; Revised Manuscript Received May 29, 1987

ABSTRACT: Interaction of an iodide ion with lactoperoxidase was studied by the use of ^{1}H NMR, ^{127}I NMR, and optical difference spectrum techniques. ^{1}H NMR spectra demonstrated that a major broad hyperfine-shifted signal at about 60 ppm, which is ascribed to the heme peripheral methyl protons, was shifted toward high field by adding KI, indicating the binding of iodide to the active site of the enzyme; the dissociation constant was estimated to be 38 mM at pH 6.1. The binding was further detected by ^{127}I NMR, showing no competition with cyanide. Both ^{1}H NMR and ^{127}I NMR revealed that the binding of iodide to the enzyme is facilitated by the protonation of an ionizable group with a pK_a value of 6.0–6.8, which is presumably the distal histidyl residue. Optical difference spectra showed that the binding of an aromatic donor molecule to the enzyme is slightly but distinctly affected by adding KI. On the basis of these results, it was suggested that an iodide ion binds to lactoperoxidase outside the heme crevice but at the position close enough to interact with the distal histidyl residue which possibly mediates electron transport in the iodide oxidation reaction.

Peroxidases (EC 1.11.1.7, donor:H_2O_2 oxidoreductase) are a family of heme-containing enzymes which catalyze the oxidation of many organic and inorganic compounds with hydrogen peroxide (Saunders et al., 1961). Of many inorganic compounds, iodide is the most attractive substrate, because it plays an important role in thyroid hormone biosynthesis and bactericidal reaction catalyzed by thyroid peroxidase and lactoperoxidase, respectively (Morrison & Schonbaum, 1976; Nunez & Pommier, 1982). However, the mechanism of oxidation of inorganic compounds by peroxidases has been less sufficiently studied so far (Dunford & Stillman, 1976), as compared with the oxidation of aromatic donor molecules catalyzed by peroxidases, especially by horseradish peroxidase.

It was reported that the oxidation of iodide with hydrogen peroxide catalyzed by thyroid peroxidase and lactoperoxidase occurs in the manner of two-electron transfer, in contrast to one-electron transfer for usual aromatic donor molecules (Magnusson et al., 1984; Ohtaki et al., 1981). The mechanism of the two-electron-transfer reaction, however, is still obscure although several views were presented. In order to elucidate the mechanism, studies on the interaction of iodide with these enzymes are needed.

Horseradish peroxidase is also known to catalyze the oxidation of iodide with hydrogen peroxide in a manner of two-electron transfer only under acidic conditions (Björkstén, 1970). The binding of iodide to horseradish peroxidase was studied by spectrophotometric (Björkstén, 1970), kinetic (Pommier et al., 1973), fluorometric (Ugarova et al., 1981), ^{127}I NMR (Sakurada et al., 1985), and ^{1}H NMR (Sakurada et al., 1987) techniques. The ^{1}H NMR studies disclosed that

† This work was supported in part by a grant-in-aid from the Ministry of Education, Science, and Culture of Japan (62580107).
‡ Chiba University.
§ Japan Women's University.
∥ Tohoku University.
⊥ Hirosaki University.

0006-2960/87/0426-6478$01.50/0